


Assessment of Metabolic Changes in *Mycobacterium smegmatis* Wild-Type and *alr* Mutant Strains: Evidence of a New Pathway of D-Alanine Biosynthesis

Darrell D. Marshall,^{†,||} Steven Halouska,^{†,||} Denise K. Zinniel,[‡] Robert J. Fenton,[‡] Katie Kenealy,[‡] Harpreet K. Chahal,[‡] Govardhan Rathnaiah,[‡] Raúl G. Barletta,^{*,‡,§} and Robert Powers^{*,†,§} 

[†]Department of Chemistry, University of Nebraska-Lincoln, Lincoln, Nebraska 68588-0304, United States

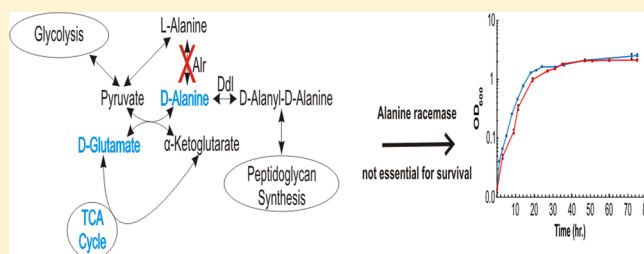
[‡]School of Veterinary Medicine and Biomedical Sciences, University of Nebraska-Lincoln, Lincoln, Nebraska 68583-0905, United States

[§]Center for Redox Biology, University of Nebraska-Lincoln, Lincoln, Nebraska 68588-0662, United States

Supporting Information

ABSTRACT: In mycobacteria, D-alanine is an essential precursor for peptidoglycan biosynthesis. The only confirmed enzymatic pathway to form D-alanine is through the racemization of L-alanine by alanine racemase (Alr, EC 5.1.1.1). Nevertheless, the essentiality of Alr in *Mycobacterium tuberculosis* and *Mycobacterium smegmatis* for cell survivability in the absence of D-alanine has been a point of controversy with contradictory results reported in the literature. To address this issue, we examined the effects of *alr* inactivation on the cellular metabolism of *M. smegmatis*. The *M. smegmatis* *alr* insertion mutant TAM23 exhibited essentially identical growth to wild-type mc²155 in the absence of D-alanine. NMR metabolomics revealed drastically distinct phenotypes between mc²155 and TAM23. A metabolic switch was observed for TAM23 as a function of supplemented D-alanine. In the absence of D-alanine, the metabolic response directed carbon through an unidentified transaminase to provide the essential D-alanine required for survival. The process is reversed when D-alanine is available, in which the D-alanine is directed to peptidoglycan biosynthesis. Our results provide further support for the hypothesis that Alr is not an essential function of *M. smegmatis* and that specific Alr inhibitors will have no bactericidal action.

KEYWORDS: NMR metabolomics, *Mycobacterium smegmatis*, *Mycobacterium tuberculosis*, alanine racemase, D-alanine biosynthesis



■ INTRODUCTION

Tuberculosis (TB) is a major global health problem, and it remains the first worldwide cause of death from an infectious disease.¹ Critical challenges to achieving the worldwide goals of disease control and elimination include the appearance of multiple and extensively drug-resistant *Mycobacterium tuberculosis* strains, synergism with HIV driving coinfections in AIDS patients, and bacillary persistence in latently infected individuals.² The cell wall of *M. tuberculosis* plays an important role in pathogenesis, and its biosynthesis is a major source of targets for the design of antimicrobial agents and attenuated mutants.^{3–5} As in other eubacteria, peptidoglycan is a critical component of the cell-wall backbone. D-Alanine is an essential building block of peptidoglycan and is required for the formation of peptidoglycan cross-links necessary to preserve cell integrity.^{3,5–9}

The main source of D-alanine in eubacteria is its conversion from L-alanine by alanine racemase (Alr), an enzyme encoded by the *alr* gene.^{3,5,8} The critical role of D-alanine in cell-wall peptidoglycan biosynthesis has identified the biosynthesis of D-alanine as an important target for the generation of new

antituberculosis drugs. Also, attenuated mutants devoid of D-alanine biosynthesis are a potential source for vaccine candidates. Thus *alr* essentiality and its role in mycobacterial physiology is core to the therapeutic value of targeting D-alanine biosynthesis. Studies on *alr* in the fast growing species *Mycobacterium smegmatis*, a useful model system for *M. tuberculosis*, rendered apparently contradictory results. In our initial reports, we found that the *M. smegmatis* *alr* insertion mutant grew without D-alanine.^{10–13} These data supported the existence of an alternative pathway of D-alanine biosynthesis in mycobacteria. However, contradictory results were reported as *M. smegmatis* and *M. tuberculosis* *alr* deletion mutants were unable to grow without D-alanine supplementation.^{14,15} These results negate the existence of an alternative endogenous pathway of D-alanine biosynthesis in both *M. smegmatis* and *M. tuberculosis*. In effect, D-alanine provided by Alr, or an external source, was reported to be an absolute requirement for the growth of *M. smegmatis* and *M. tuberculosis*. A rationale for the

Received: October 5, 2016

Published: January 25, 2017

observed difference in the essentiality of *M. smegmatis* *alr* was attributed to the deletion mutant being a superior construct to the insertion mutant. This explanation was based on an inferred residual Alr activity despite evidence of the contrary.^{10–13} Furthermore, the argument ignores the fact that the insertion mutant was generated by the insertion of a drug marker that split *alr* approximately in the middle of the gene,¹¹ a procedure similar to the creation of null mutant strains by transposon mutagenesis.¹⁶ Importantly, the deletion and insertion mutants were also selected and tested under different culture conditions that may impact D-alanine auxotrophy. Moreover, our recent studies on the mechanism of action of D-cycloserine (DCS) in both *M. smegmatis* and *M. tuberculosis* support our prior conclusions that Alr is nonessential and that D-alanine ligase is the lethal target of DCS in both mycobacterial species.^{10–13}

Resolution of the controversy surrounding *alr* conditional essentiality in mycobacteria is important, not only in the context of the role of Alr but also for its implications in the design of more effective drugs and vaccines targeting the endogenous synthesis of D-alanine in *M. tuberculosis*. Additionally, evidence of horizontal gene transfer in mycobacteria^{17,18} highlights the impact that the potential transfer of genes involved in an alternative pathway of D-alanine biosynthesis in a nonpathogenic species such as *M. smegmatis* might have on TB epidemiology and management. To address this issue, we undertook an NMR metabolomics study to determine whether D-alanine could be exchanged into the metabolic pool of the *M. smegmatis* *alr* insertion mutant TAM23. We report conclusive evidence of this exchange that suggests an alternative pathway of D-alanine biosynthesis in *M. smegmatis*.

MATERIALS AND METHODS

Bacterial Strains and Culture Conditions

Bacterial strains used in this study were *M. smegmatis* wild-type mc²155¹⁹ and *alr* mutant TAM23.¹¹ For all experiments, strains were grown to an OD₆₀₀ of 0.6 to 1.0 at 37 °C with shaking at 200 rpm in Middlebrook 7H9 complete media (MADC) supplemented with 0.2% (v/v) glycerol, 0.05% Tween 80, 0.01% cycloheximide, and ADC (0.5% bovine serum albumin (BSA) fraction V, 0.01 M glucose, and 0.015 M NaCl). Cycloheximide is a protein synthesis inhibitor, which was used to suppress the growth of yeast in the bacterial cell cultures. When necessary, cultures were supplemented with 50 mM D-alanine. For growth curve analysis, all cultures were inoculated to a starting OD₆₀₀ of ~0.01, and the generation times were determined as previously described.²⁰

Proteomics Sample Preparation and Data Collection

All mc²155 and TAM23 cultures (50 mL) were grown to an OD₆₀₀ of 0.8 to 1.1 in MADC media without D-alanine. The bacteria were removed, stored on ice for 10 min, and centrifuged at 3000 rpm at 4 °C for 15 min. The supernatant was removed from the cell pellet, filtered, and placed at –80 °C. Two washes with 30 mL of ddH₂O were performed, and the pellet was resuspended for a final volume of 1.0 mL in 50 mM ammonium bicarbonate containing 8 M urea and 1.5 mM phenyl-methyl-sulfonyl fluoride as a protease inhibitor. Cell lysis in the MP Biomedicals FastPrep-24 was performed three times for 20 s with a 5 min chill period between cycles. Two cycles of centrifugation were performed to remove cell debris. Protein (0.5 to 1 mg) was precipitated with cold acetone. Samples were vortexed and incubated overnight at –20 °C. Samples were then warmed to room temperature and pelleted

by centrifugation at 14 000g for 20 min, and the supernatant was discarded. After air-drying for 15–30 min, samples were subjected to MudPIT analysis at the University of Nebraska-Lincoln (UNL) Redox Biology Center Proteomics and Metabolomics Core Facility. A protease and trypsin digest was performed on the protein mixtures and then subjected to liquid chromatography electrospray mass spectrometry LC–ESI–MS. Protein identification was performed by a Mascot database search.²¹

NMR Metabolomics Sample Preparation

General procedures for the handling and preparation of *M. smegmatis* NMR samples for metabolomics analysis have been described elsewhere.²² Metabolomics samples for 1D ¹H NMR experiments were prepared from 10 replicates of both *M. smegmatis* mc²155 and TAM23 cell cultures. *M. smegmatis* mc²155 and TAM23 strains were grown at 37 °C with shaking at 200 rpm in 50 mL of MADC media in a 250 mL flask for 10–12 h until an OD₆₀₀ of 0.6 to 1.0. A second set of 10 replicate cultures per strain was grown under the same condition with the exception that the TAM23 cultures were supplemented with 50 mM D-alanine after the OD₆₀₀ reached ~0.6. All of the bacterial cultures were then allowed to grow for an additional 2 h. The cell cultures were placed on ice for 5 min and kept on ice throughout the entire process of metabolome extraction. Bacterial cells were harvested by centrifugation at 2000g at 4 °C for 15 min in 50 mL tubes. The cells were washed twice with 30 mL of ice-cold double-distilled water. The cell pellets were resuspended with 1.0 mL of double-distilled water and transferred to a 2 mL vial containing 0.1 mm silica beads (Lysing Matrix B). The cells were then lysed for 40 s at 6 m/s using a MP Biomedicals FastPrep-24. The cell lysate was centrifuged for 10 min at 12 400g and 4 °C. The supernatant was extracted and then lyophilized and resuspended with 1.0 mL of 100% D₂O containing 50 mM phosphate buffer (uncorrected pH 7.2) with 50 μM 3-(trimethylsilyl) propionic-2,2,3,3-*d*₄ acid sodium salt (TMSP). The samples were vortexed and then centrifuged. A 600 μL portion of the cell free extract was then transferred to an NMR tube. A total of 40 metabolomics samples were prepared for collecting 1D ¹H NMR spectra.

NMR metabolomics samples for 2D ¹H–¹³C HSQC experiments were prepared from triplicate *M. smegmatis* mc²155 and TAM23 cultures grown in 110 mL of MADC media (250 mL flasks). The bacterial cultures were grown at 37 °C with shaking at 200 rpm for 10–12 h until an OD₆₀₀ of ~0.6. The culture media was then supplemented with or without 100 μM [¹³C₂]-D-alanine, and the cultures were allowed to grow for an additional 2 h. The bacterial cells were processed and the metabolome was extracted following the same protocol described above.

NMR Data Collection

The NMR data were collected and processed according to our previously described protocol.²³ The NMR spectra were collected on a Bruker Avance DRX 500 MHz spectrometer equipped with a 5 mm triple-resonance cryogenic probe (¹H, ¹³C, ¹⁵N) with a z-axis gradient, BACS-120 sample changer, and an automatic tuning, and a matching accessory was utilized for automated NMR data collection. 1D ¹H NMR spectra were collected with Purge solvent saturation,²⁴ a ¹H 90° pulse of 8 μs, and a spectral width of 5482.5 Hz and 32k data points at 298 K. A total of 16 dummy scans and 128 scans were used

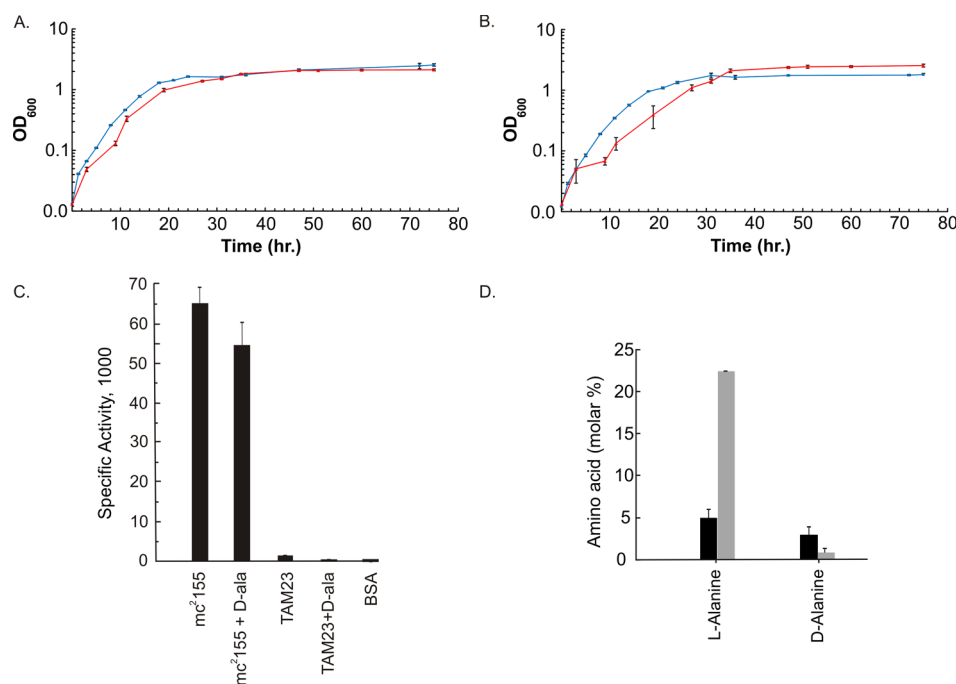


Figure 1. Growth curves for wild-type *M. smegmatis* mc²155 cells (blue) or *alr* mutant TAM23 cells (red) treated (A) without D-alanine or (B) with 50 mM D-alanine, respectively. Growth curves were collected in triplicate and the error bars were calculated using SEM. (C) Mean specific activities (μmoles of substrate consumed per min per mg protein) in *M. smegmatis* cell extracts. Data are as described previously by Chacon et al. 2002.¹¹ Cells were grown to midexponential phase, harvested, and lysed. Cell-free extracts were assayed for Alr activity in triplicate. A bovine serum albumin (BSA) control was prepared at the same protein concentration as the cell extracts and assayed in triplicate. All error bars were calculated using standard deviations. (D) Intracellular steady-state concentrations of amino acids L- and D-alanine in mc²155 (black) and TAM23 (gray). Data reproduced with permission from ref 10. Copyright 2009 Microbiology Society.

with a recycle delay of 1.5 s for a total acquisition time of 10 min per spectrum.

A series of three time-zero 2D ¹H–¹³C HSQC spectra (HSQC₀) were collected using the pulse sequence described by Hu et al. for determination of absolute metabolite concentration changes.^{25,26} The NMR spectra were collected with 2048 data points and a spectral width of 5000.0 Hz in the direct ¹H dimension and 64 data points and a spectral width of 17605.6 Hz in the indirect ¹³C dimension. A total of 16 dummy scans and 64 scans with a relaxation delay of 1.5 s were used to obtain each 2D ¹H–¹³C HSQC₀ spectrum with a total acquisition time of 6 h.

Multivariate Statistical Analysis

The 1D ¹H NMR spectra were processed in our MVAPACK software suite (<http://bionmr.unl.edu/mvapack.php>).²⁷ For principal component analysis (PCA), the 1D ¹H NMR spectra were processed with a 1.0 Hz exponential apodization function, followed by Fourier transformation, automatic phasing, and normalization with phase-scatter correction (PSC),²⁸ and referenced to TMS-PD₄ (0.0 ppm). The noise- and solvent-containing regions were manually removed, and the spectrum was binned using an adaptive intelligent binning algorithm²⁹ and Pareto-scaled. For orthogonal projections to latent structures discriminant analysis (OPLS-DA), the NMR data were processed using MVAPACK as described above. The table of integrals was center-averaged and imported into SIMCA version 13.0 (Umetrics) to produce the S-plots. Supervised classification for each group was determined by cell type, with *M. smegmatis* mc²155 defined as the control (or assigned a value of 0) and *M. smegmatis* TAM23 assigned a value of 1. Ellipses were generated for each group in the PCA scores plot using our

PCA/PLS-DA utilities.^{30,31} The ellipses correspond to the 95% confidence limits of a normal distribution for each group.

Metabolite Identification and Measurement of Absolute Concentration Changes

2D ¹H–¹³C HSQC spectra were processed using NMRPipe.³² The spectra were Fourier-transformed, manually phased, and baseline-corrected. The processed 2D ¹H–¹³C HSQC spectra were then analyzed using NMRView³³ to assign chemical shifts, intensities, and volumes to each NMR resonance. Chemical shift lists were assigned to specific metabolites using the Human Metabolome Database,³⁴ Madison Metabolomics Database,³⁵ and the Platform for Riken Metabolomics.³⁶ A chemical shift error tolerance of 0.05 and 0.40 ppm was used for ¹H and ¹³C chemical shifts, respectively. The identification of metabolites and metabolomics pathways from the NMR metabolomics data was further verified using the Kyoto Encyclopedia of Genes and Genomes (KEGG)³⁷ and MetaCyc³⁸ databases.

Metabolite peak volumes from the HSQC₀ experiment were calculated as previously described.^{25,26} In brief, peak volumes from a 2D ¹H–¹³C HSQC experiment are dependent on the magnitude of J-coupling constants, relaxation processes, dynamics, and metabolite concentrations. The HSQC₀ experiment is a series of three HSQC experiments with an increasing number of HSQC pulse sequence repetitions (i.e., HSQC₁, HSQC₂, HSQC₃). In this manner, the HSQC peak volume will decrease proportional to the number of pulse sequence repetitions due to the impact of all factors except concentration. A natural log plot of peak volumes versus the increment number (1, 2, 3) allows for the extrapolation back to increment 0 or zero-time, which is proportional to the metabolite's

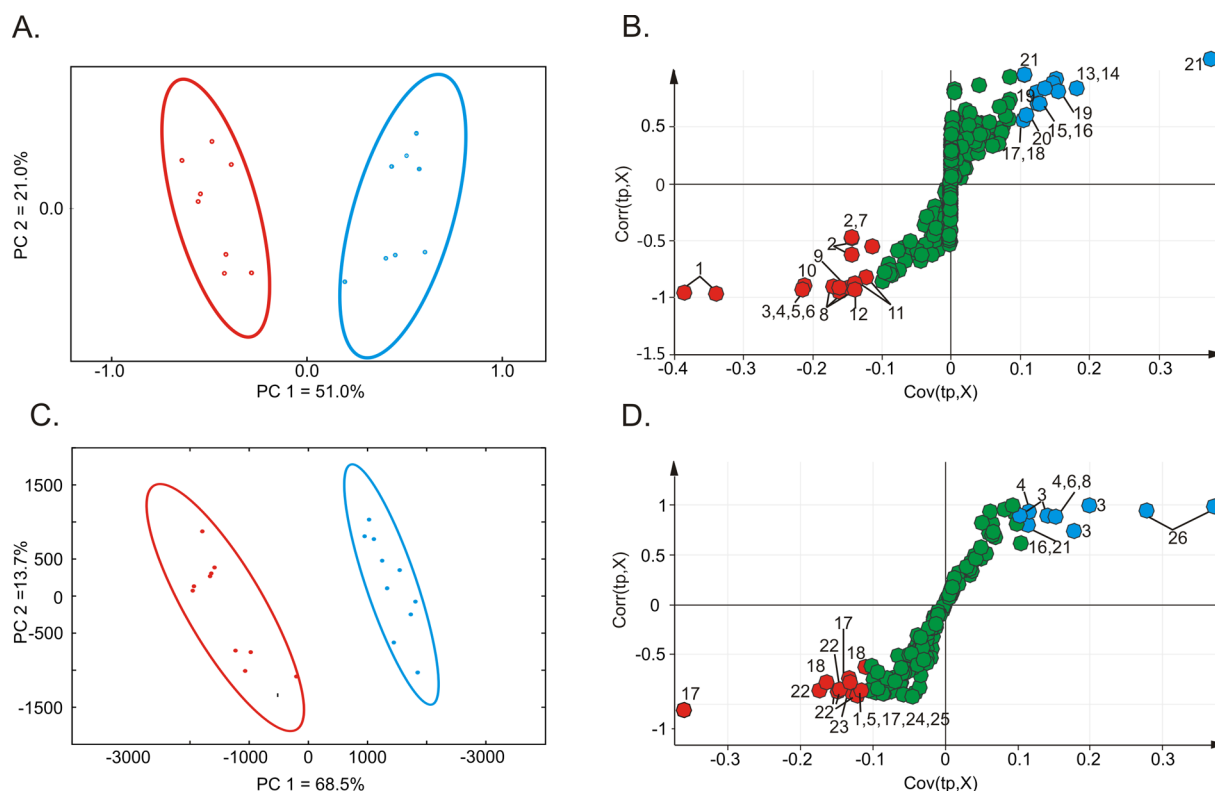


Figure 2. PCA scores plots generated from 1D ^1H NMR spectra obtained from *M. smegmatis* TAM23 (red) and mc^2155 (blue) cell lysates (A) without or (C) with media supplemented with D-alanine. OPLS-DA S-plots comparing the 1D ^1H NMR spectra obtained from TAM23 and mc^2155 cell lysates (B) without or (D) with media supplemented with D-alanine. Each point in the S-plot represents a specific bin of integrals for a chemical shift range of 0.25 ppm. The points at the extreme ends of the S-plots are major contributors to class distinction. The red points represent a decrease in the binned integrals for TAM23 compared with mc^2155 . The blue points represent an increase in the binned integrals for TAM23 compared with mc^2155 . Green points represent metabolites that are approximately equally in both strains. The labeled points were assigned to the following metabolites: (1) fatty acids, (2) ethanol, (3) glutamate, (4) oxaloacetate, (5) GABA, (6) succinate, (7) glycerol, (8) isoleucine, (9) valerate, (10) lactate, (11) N-acetylglucosamine-6-phosphate, (12) α -ketoisovalerate, (13) glycolate, (14) serine, (15) phosphoserine, (16) threonine, (17) lysine, (18) alanine, (19) glucarate, (20) ATP, (21) unidentified (UD), (22) trehalose, (23) valine, (24) ornithine, (25) α -ketoglutarate, and (26) citrulline.

concentration. The calibration of metabolite peak volumes from the HSQC₀ experiments with an absolute concentration was calculated with a standard calibration curve as previously described.²³ In brief, five different mixtures containing nine different ^{13}C -labeled metabolites (2-keto-3-methylbutyrate, 2-ketobutyrate, acetate, alanine, fructose, glucose, glycine, pyruvate, succinate) with a range of known concentrations (5 to 300 μM) were used to collect a series of HSQC₀ experiments. The HSQC₀ peak volumes were determined for each metabolite at each concentration, as described above. The HSQC₀ peak volumes were then plotted versus the known metabolite concentrations to yield a standard calibration curve. The triplicate HSQC₀ experiments were used to calculate averages and standard deviations for each metabolite concentration.

RESULTS

Growth Curves of *M. smegmatis* *alr* Mutants

When grown in MADC, the wild-type and the *alr* insertion mutant were still able to proliferate in the absence of D-alanine. In our original studies, we observed that TAM23 grew with a significant lag time when subcultured from an inoculum grown in media with D-alanine. However, in this study we subcultured from inocula prepared after the cells were passaged in media without D-alanine. Under these conditions, both strains yielded growth curves that followed similar trends (Figure 1A). Strains

mc^2155 and TAM23 grew with a generation time of 208 ± 34 and 294 ± 29 min, had an initial lag phase of 5 and 12 h, and reached saturation densities (OD₆₀₀) of 2.5 and 2.1, respectively. A similar result was obtained for both strains when the media was supplemented with D-alanine except for a moderately higher saturation density for TAM23 (Figure 1B). Strains mc^2155 and TAM23 had generation times of 310 ± 28 and 294 ± 33 min, lag phases of 4 and 6.5 h, and saturation densities of 1.7 and 2.54, respectively. When comparing the growth curves with and without D-alanine, TAM23 was able to grow more efficiently in the presence of D-alanine, while the opposite was true for mc^2155 . Even though the slopes during the exponential phase of growth are significantly different (p value < 0.001) when comparing TAM23 grown in no D-alanine to mc^2155 grown with and without D-alanine and TAM23 with D-alanine, there does not appear to be a biological difference. These results demonstrate that the *alr* gene is not essential for the survivability of *M. smegmatis* in the absence of D-alanine and that an alternative pathway for synthesizing D-alanine must exist.

Major Proteomic Changes in *M. smegmatis* *alr* Mutants

MudPIT analysis identified 904 proteins expressed in media without D-alanine. TAM23 protein overexpression was defined as a 10-fold or greater expression level relative to mc^2155 . Thirty-one proteins were identified as being overexpressed in TAM23 relative to mc^2155 (Supplemental Table S1). Several

enzymes directly involved in central carbon metabolism were affected by the *alr* mutation. Specifically, alanine dehydrogenase (ALD) and several alcohol dehydrogenases (ADHs) were all overexpressed in TAM23. The ADH enzymes exhibited an approximate 40-fold increase in TAM23 relative to mc²155. Similarly, ALD was upregulated by ~30-fold in TAM23.

Metabolic Impact of Media Lacking D-Alanine on *M. smegmatis* *alr* Mutants

The set of 1D ¹H NMR spectra were used to assess the global metabolome differences between wild-type *M. smegmatis* mc²155 and the alanine racemase TAM23 insertion mutant (Figure S1). The PCA scores plot (Figure 2A) compares the metabolomes of *M. smegmatis* mc²155 cells and the TAM23 insertion mutant grown in MADC without D-alanine. The scores plot reduces the complex 1D ¹H NMR spectrum that captures the state of the cellular metabolome into a single point in principal component space (PC1, PC2, etc.). Correspondingly, the principal components represent the largest variations between the individual 1D ¹H NMR spectra. The scores plot indicates that PC1 and PC2 account for 51.0 and 21.0% of the variation in the NMR spectra, respectively. A total of 10 replicates for the wild-type mc²155 and the *alr* TAM23 insertion mutant form two distinct clusters in the PCA scores plot. The unsupervised PCA model demonstrates a statistically significant difference between the metabolomes of *M. smegmatis* wild-type mc²155 cells and the *alr* TAM23 insertion mutant.

An OPLS-DA model was generated from the metabolomics data sets to further characterize the mc²155 and TAM23 metabolome and to identify the discriminatory variations that maximize group separation.³⁹ The OPLS-DA model without the addition of D-alanine yielded a reliable fit, as evident by an R_x^2 of 0.652, R_y^2 of 0.971, and a Q^2 of 0.923 (Figure S2A). Importantly, cross-validation using CV-ANOVA produced a statistically significant p value of 5.17×10^{-6} , indicating a valid OPLS-DA model. The group separation between the alanine racemase TAM23 mutant and the mc²155 wild-type metabolomes is statistically significant, which is consistent with the group separation observed in the PCA scores plot. Furthermore, an S-plot generated from the OPLS-DA model identified the NMR spectral differences and, correspondingly, the major metabolome changes contributing to the group separations in the scores plot (Figure 2B). The variables (chemical shifts) with a large modeled correlation [approximately 1 (correlated) or -1 (anticorrelated)] and large modeled covariation ≥ 0.1 or ≤ -0.1 were identified as key contributors to group separations in the OPLS scores plot and are labeled on the S-plot. The metabolites from the S-plot identified as major contributors to group separation in the absence of supplemental D-alanine are summarized in Table 1.

Impact of D-Alanine on the Metabolome of *M. smegmatis* *alr* Mutants

The NMR metabolomics experiment was repeated using *M. smegmatis* mc²155 and TAM23 cells grown in MADC supplemented with 50 mM D-alanine. As previously observed, the PCA scores plot contained two distinct clusters, indicating a difference between the mc²155 and TAM23 metabolomes (Figure 2C). PC1 and PC2 account for 68.5 and 13.7% of the variation in the data, respectively.

The OPLS-DA scores plot exhibited a similar group separation between *M. smegmatis* mc²155 wild-type cells and the TAM23 *alr* mutant (Figure S2B). The OPLS-DA yielded a reliable fit as evident by R_x^2 of 0.682, R_y^2 of 0.981, and a Q^2 of

Table 1. Relative Differences in Metabolite Concentrations between *M. smegmatis* Wild-Type and TAM23 *alr* Mutant Cells

no D-alanine ^{a,b}		50 mM D-alanine	
relative increase	relative decrease	relative increase	relative decrease
	α -ketoisovalerate	citrulline	alanine
alanine	ethanol	fatty acid	α -ketoglutarate
fatty acid			
ATP	GABA	glutamate	GABA
	glutamate	isoleucine	lysine
glucarate	glycerol	oxaloacetate	ornithine
glycolate	isoleucine	succinate	trehalose
lysine	lactate	threonine	valine
phosphoserine	N-acetyl-glucosamine-6-phosphate		
serine	oxaloacetate		
threonine	succinate		
	valerate		

^aObserved increase or decrease in metabolite concentrations in *M. smegmatis* TAM23 *alr* mutant cells relative to wild-type mc²155 cells. Metabolites were identified from the S-plots generated from the corresponding OPLS-DA model (see Figure 2). ^bMetabolites in italics exhibited a reversal in concentration depending on whether media were supplemented with or without D-alanine.

0.957. Importantly, cross-validation using CV-ANOVA produced a statistically significant p value of 4.39×10^{-10} , indicating a valid OPLS-DA model. The group separation between the alanine racemase TAM23 mutant and the mc²155 wild-type metabolomes is statistically significant, which is consistent with the group separation observed in the PCA scores plot. The S-plot from OPLS-DA model was used to identify the chemical shifts (metabolites) that significantly contributed to the group separation in the OPLS-DA scores plot (Figure 2D). The metabolites from the S-plot identified as major contributors to group separation in the presence of supplemental D-alanine are summarized in Table 1.

Quantitative Analysis of Metabolite Changes in *M. smegmatis* *alr* Mutants

The NMR metabolomics experiment was repeated using *M. smegmatis* mc²155 and TAM23 cells grown in MADC supplemented with 100 μ M of ¹³C-labeled [¹³C₂]-D-alanine. Triplicate sets of ¹³C-labeled metabolite extracts were prepared per strain and then analyzed using time-zero ¹H-¹³C HSQC (HSQC₀) experiments.^{25,26} A 2D ¹H-¹³C HSQC NMR spectrum allows for easier identification of metabolites because of the reduced complexity and spectral overlap compared with a 1D ¹H NMR spectrum. Only metabolites that originate from the supplemental ¹³C-D-alanine are observed in the 2D ¹H-¹³C HSQC spectrum (Figure S3). Each peak in the 2D ¹H-¹³C represents a ¹³C-¹H pair for a specific metabolite that were assigned by matching the chemical shifts against NMR metabolomics databases.³⁴⁻³⁶ A total of 38 metabolites were identified from the two *M. smegmatis* strains.

A concentration for each metabolite was determined by extrapolating peak volumes from a series of three 2D ¹H-¹³C HSQC spectra at different time points to interpolate a time-zero peak volume. The spectra were collected in triplicate to determine an average peak volume and calculate a standard deviation. The average time-zero peak volume is directly proportional to a concentration based on a calibration curve

using 9 ^{13}C -labeled compounds of known concentration.²³ A plot of the absolute metabolite concentrations for the *M. smegmatis* mc²155 and TAM23 strains is shown in Figure 3.

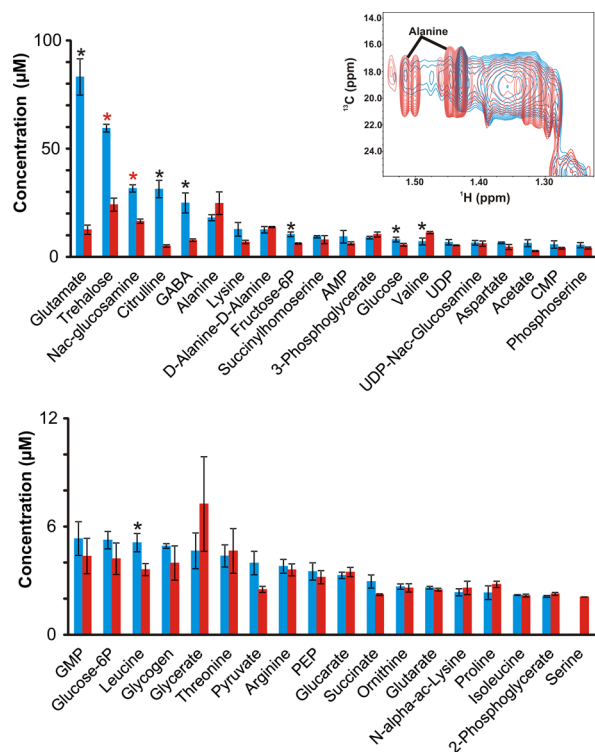


Figure 3. Bar graph summarizing metabolite concentrations determined from 2D ^1H - ^{13}C HSQC₀ experiments. *M. smegmatis* mc²155 (blue) and TAM23 (red) cell cultures were supplemented with 100 μM ^{13}C -labeled [$^{13}\text{C}_2$]-D-alanine. Statistical significance at the 95% confidence level is denoted by a black asterisk, and a red asterisk indicates a statistical significance after applying Bonferroni multiple hypothesis correction. (insert) Expanded view of an overlay of the wild-type strain mc²155 (blue) and *alr* insertion mutant TAM23 (red) 2D ^1H - ^{13}C HSQC₀ spectra highlighting alanine concentration changes. The full spectral overlay is in the Supporting Information (see Figure S3).

Peptidoglycan precursors such as glutamate, lysine, and N-acetyl-glucosamine were significantly decreased in the *alr* insertion mutant. The concentration of trehalose, an essential precursor for trehalose-containing glycolipids, which allows the attachment of glycolipids to arabinogalactan in the cell wall was also decreased in the *alr* insertion mutant.⁴⁰

DISCUSSION

Multiple resistant strains of TB are growing and spreading at a rapid pace, and the concurrent loss of antibiotic efficacy is predicted to cause upward of 10 million deaths annually by 2050. Avoiding this potential pandemic requires developing new antibiotics that circumvent common mechanisms of resistance, which necessitates the identification of novel therapeutic targets. For antibiotics, therapeutic targets have commonly been an essential enzyme or protein. Alr is a pyridoxal 5'-phosphate (PLP)-containing enzyme that is thought to be necessary for the growth of mycobacteria.^{41–43} The racemization of L-alanine to D-alanine by Alr is the only confirmed enzymatic reaction in *M. tuberculosis* or *M. smegmatis* to produce the D form of alanine, which is an essential

intermediate for peptidoglycan biosynthesis.⁸ Nevertheless, the essentiality of Alr in *M. smegmatis* and *M. tuberculosis* survivability and its significance as a therapeutic target have been highly controversial.

Chacon et al. previously observed that an *alr* knockout mutant (TAM23) was able to grow under conditions without supplementing D-alanine into Middlebrook 7H9 or minimal medium.^{10,11} The TAM23 strain did not exhibit any growth defects, but it was clear that the phenotypic changes between TAM23 and the wild-type strain were pronounced.^{10,11} Again, we did not observe any biologically significant differences when we compared the TAM23 growth curve, upon passage for growth in media without D-alanine, to the wild-type mc²155 strain in the absence of D-alanine (Figure 1A). In fact, we observed a higher saturation density for the TAM23 growth curve relative to mc²155 with the addition of D-alanine to the culture media (Figure 1B). One potential interpretation is that the stress response TAM23 experiences due to the lack of both *alr* activity and D-alanine is partly relieved by supplemented D-alanine, leading to a relative improvement in cell growth. Regardless, TAM23 does not exhibit any growth defects in the absence or presence of D-alanine, strongly implying that the *alr* inactivation does not negatively impact cell survivability. This is in direct conflict with other studies that show Alr to be essential in mycobacteria.^{14,15} These discrepancies may be attributed to contrasting mutant construction and cell growth conditions. TAM23 is an insertion mutant, which still has the potential of producing a protein product with residual or defective activity. However, as discussed above, this possibility is extremely unlikely as the insertion mutation would be similar to a transposon insertion in the middle of the gene. Furthermore, we previously examined Alr activity in TAM23 and did not detect any activity above BSA background (Figure 1C).¹⁰ The lack of Alr activity in TAM23 was also supported by examining the steady-state concentrations of L- and D-alanine. L-Alanine was observed to accumulate in TAM23, which is consistent with an inactive Alr (Figure 1D). Conversely, the D-alanine production in TAM23 was below that of mc²155 but still above background levels. This is consistent with the *alr* mutant producing D-alanine through an alternative mechanism. Recently, we proposed an alternative metabolic pathway for the production of D-alanine in *M. tuberculosis* and *M. smegmatis* to compensate for an inactive Alr.^{12,13} An alternative source of D-alanine may result from an unidentified transaminase converting pyruvate into D-alanine. This hypothesis resulted from a metabolomics investigation into the in vivo lethal target of DCS, in which Alr and D-alanine-D-alanine ligase (Ddl) had been previously identified as likely targets for DCS. We identified Ddl as the in vivo lethal target of DCS based on an observed decrease in the biosynthesis of D-alanyl-D-alanine that occurred simultaneously with a DCS-induced inhibition on cell growth. We also previously observed that the incorporation of ^{13}C -carbons from D-alanine into glutamate was dependent on DCS concentration, which strongly suggests a transaminase compensating for an inactive Alr.

Herein, we further tested our hypothesis that Alr is nonessential for peptidoglycan biosynthesis and the survivability of *M. smegmatis* by examining the total proteomic and metabolic shifts that occur in TAM23 relative to wild-type mc²155 cells. Our proteomics analysis revealed that ALD and ADH enzymes were significantly overexpressed from Alr inactivation. Of particular note, ALD is involved in a metabolic recycling process, which includes an alternative pathway for the

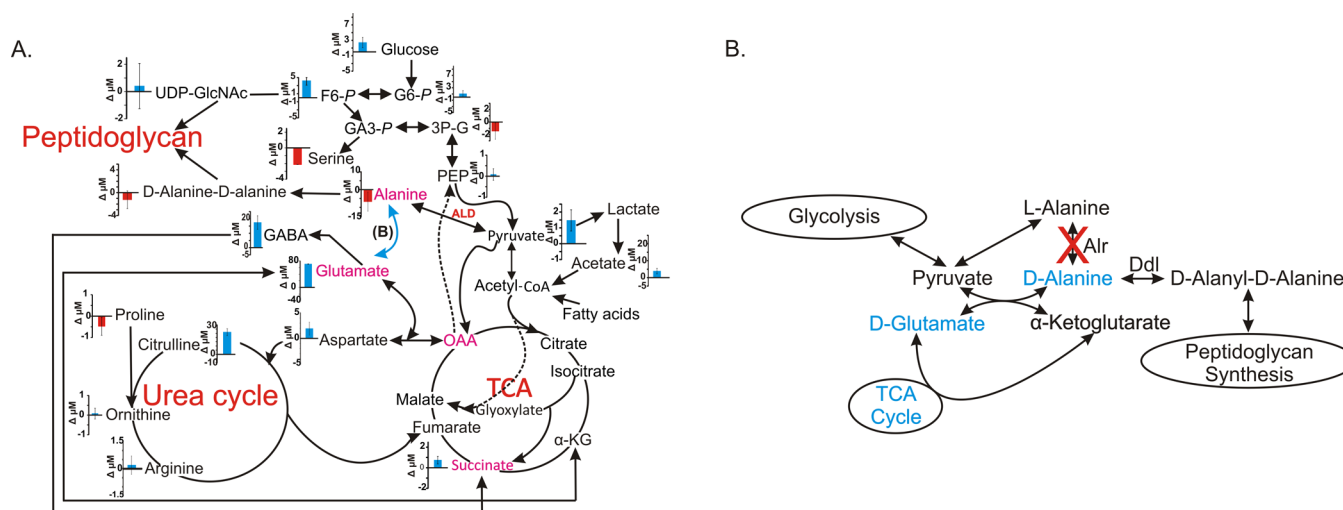


Figure 4. (A) Metabolic network map displays the 2D ^1H - ^{13}C -HSQC time zero absolute metabolite concentration differences between *M. smegmatis* wild-type mc²155 and *alr* insertion mutant TAM23 grown in MADC media and treated at midexponential phase with [$^{13}\text{C}_2$]-D-alanine. A positive blue bar indicates a concentration increase in mc²155 relative to TAM23. A negative red bar indicates a concentration decrease in mc²155 relative to TAM23. The plotted concentrations are on a micromolar scale and the error bars represent standard deviations. Metabolites highlighted in magenta exhibited a reversal in concentration depending on whether media were supplemented with or without D-alanine from the 1D ^1H NMR experiments and Table 1. L-Alanine dehydrogenase (ALD), highlighted in red, was overexpressed in TAM23 relative to mc²155. The dark arrows identify the primary carbon flux pathway, blue arrows represent a hypothetical pathway for D-alanine biosynthesis that is depicted in detail in panel B, and the dotted lines represent established alternative routes. (B) Metabolic network summarizing the 1D ^1H NMR data and the L-D amino acid pools (see Figure 1D and Table 1) comparing mc²155 with TAM23 from cultures without supplemental D-alanine. Metabolites colored blue were observed to increase in mc²155 relative to TAM23. Diagram adapted from ref 51.

biosynthesis of D-alanine. ALD catalyzes the oxidative deamination of L-alanine to produce pyruvate and ammonia with concomitant formation of NADH.⁴⁴ Thus ALD may provide an alternative source of D-alanine via pyruvate, where pyruvate and D-glutamate are then converted into D-alanine and α -ketoglutarate by a transamination reaction. A D-amino acid aminotransferase (Dat) capable of catalyzing this transamination reaction has been previously observed in *Bacillus subtilis*, *Listeria monocytogenes*, and numerous other bacteria.^{45–50} While not verified, we previously identified a number of enzymes that may potentially perform the same function in *M. smegmatis*.⁵¹ In the absence of supplemental D-alanine, the overproduction of ALD in TAM23 increases the reducing potential (generation of NADH). This is compensated for by the overproduction of ADH enzymes to regenerate NAD through the oxidation of NADH. Thus this metabolic change is necessary to maintain redox balance when Alr is inactive.

The increase in ammonia production from an elevated ALD activity did not lead to an observable toxicity for *M. smegmatis*. In fact, ammonia is a preferred source of nitrogen for *M. smegmatis* and is a diffusible substance that participates in many metabolic processes and consequently is under tight regulatory control.⁵²⁻⁵⁴ There is always a balance of oxidative deaminations and reductive aminations. Furthermore, there are outer membrane proteins that participate in the influx and efflux of ammonia. As a result, *M. smegmatis* is readily able to adapt to large variations in nitrogen (ammonia) availability through a variety of cellular processes. Similarly, the increase in ADH activity to regenerate NAD would be expected to increase the conversion of an acetaldehyde to an alcohol, which is then excreted from the cell. This is also consistent with the prior observation that *M. smegmatis* ADH has a preference to function as an aldehyde reductase and convert acetaldehydes into alcohols.⁵⁵

From a 1D ^1H NMR metabolomics study we observed statistically significant differences between the mc²155 and TAM23 metabolomes based on the distinct clusters in the PCA scores plot (Figure 2A). The metabolite changes identified from the resulting S-plot (Figure 2B) are listed in Table 1. As previously observed, the difference in the mc²155 and TAM23 metabolomes was eliminated when TAM23 was complemented with the wild-type *alr* gene.¹² Conversely, supplementing the culture media with D-alanine had no effect; the mc²155 and TAM23 global metabolomes are still significantly different (Figures 2C,D and Table 1). The pronounced difference in the mc²155 and TAM23 metabolomes and the inability of supplemental D-alanine to reverse these metabolic differences eliminates the hypothesis that TAM23 is able to survive in the absence of D-alanine due to residual or defective *Alr* activity. Instead, the metabolic differences persist because a clear switch in the metabolic state of TAM23 ensues when TAM23 is cultured in the presence or absence of D-alanine. TAM23 cells enter an anabolic state when D-alanine is not readily available. Intriguingly, when D-alanine is available to TAM23, we observe a complete reversal in the flow of carbon through some metabolic processes. In effect, the addition of D-alanine circumvents the need for a metabolic response to replace the missing D-alanine due to the *alr* inactivation. Instead, TAM23 simply directs the D-alanine into peptidoglycan biosynthesis, which then allows the cell to pursue normal metabolic processes. Nevertheless, TAM23 still exhibits a distinct metabolism compared with mc²155. For instance, fatty acids are increased in TAM23 relative to mc²155, presumably to redirect fatty acids to increase cell-wall integrity. The metabolites that exhibited a reversal in cellular concentrations based on the availability of D-alanine are colored in the metabolic pathways in Figure 4. Indeed, supplementation with D-alanine induced a metabolic switch for TAM23, as revealed by the 1D ^1H NMR metabolomics experiments (Figure 4B).

To further evaluate the metabolic response due to *alr* inactivation, we traced the distribution of ^{13}C -carbon derived from $[\text{C}_2^{13}]$ -D-alanine throughout the TAM23 and mc²155 metabolome using 2D ^1H - ^{13}C HSQC NMR experiments (Figures 3 and 4A). In *M. tuberculosis* and *M. smegmatis*, D-alanine can be directly converted into L-alanine (by Alr), into D-alanyl-D-alanine (by Ddl), into pyruvate (by an unidentified transaminase), or into alanyl-poly(glycerolphosphate)/D-alanine-poly(phosphoribitol). As expected, *alr* inactivation causes more of the supplemented D-alanine to be biosynthesized into D-alanyl-D-alanine in TAM23 relative to mc²155. More notably, a drastic decline is observed in the conversion of D-alanine into glutamate and pyruvate along with an accumulation of $[\text{C}_2^{13}]$ -D-alanine in TAM23. This is consistent with an inactive Alr in TAM23 that prevents the D-alanine carbon from entering into other metabolic pathways besides peptidoglycan biosynthesis. In fact, a likely pathway is the conversion of D-alanine into pyruvate by the unidentified transaminase, which, apparently, is significantly less efficient than Alr in directing the supplemental D-alanine into central carbon metabolism. Conversely, the supplied D-alanine is not essential to peptidoglycan biosynthesis in mc²155 because Alr is still active. Instead, D-alanine can be used as an alternative carbon source by converting it into L-alanine, which is then diverted into other metabolic processes. We observed an increase in the conversion of $[\text{C}_2^{13}]$ -D-alanine into glucose, fructose-6-phosphate, pyruvate, glutamate, GABA, succinate aspartate, and citrulline for mc²155 (Figures 3 and 4A). This indicates an increase in the flow of carbon through glycolysis, the TCA cycle, and urea cycle, with a simultaneous decrease from peptidoglycan biosynthesis. Notably, the 1D ^1H NMR experiments indicate an increase in the cellular concentration of citrulline, glutamate, and succinate for TAM23 with supplemental D-alanine. This apparent discrepancy highlights the fact that the different NMR experiments actually measure two distinctly different metabolic changes. The 1D ^1H NMR experiments measure the total pool of these metabolites within the cell culture regardless of the carbon source. Conversely, the 2D ^1H - ^{13}C HSQC experiment is only measuring the amount of citrulline, glutamate, and succinate derived from the supplied $[\text{C}_2^{13}]$ -D-alanine. The observed changes in the concentrations of GABA and glutamate for TAM23 may also be indicative of a stress response resulting from an inactive Alr in our mutant strain especially in conditions without D-alanine.⁵⁶ The decrease in GABA and glutamate derived from $[\text{C}_2^{13}]$ -D-alanine are consistent with D-alanine being shunted into other critically needed metabolites, where other carbon sources may be used for GABA and glutamate production.

CONCLUSIONS

Taken together, these new data uniformly agree with the hypothesis of an inactive Alr in TAM23 and an alternative transaminase as a source of D-alanine for TAM23 (Figure 4). Our results further confirm that Alr is not an essential enzyme in *M. smegmatis*. Because central metabolic pathways are conserved in mycobacteria, these results also suggest that Alr is not essential in *M. tuberculosis* and that Alr inhibitors will not have a bactericidal action.

ASSOCIATED CONTENT

Supporting Information

The Supporting Information is available free of charge on the ACS Publications website at DOI: 10.1021/acs.jproteome.6b00871.

Table S1. Proteins exhibiting a significant change in expression levels between TAM23 and mc²155 cells cultured in media without D-alanine. Figure S1. Representative examples of 1D ^1H NMR spectra of *M. smegmatis* metabolite extracts. Figure S2. OPLS-DA model generated from the 1D ^1H NMR spectra obtained from *M. smegmatis* metabolite extracts. Figure S3. Overlay of 2D ^1H - ^{13}C HSQC spectra generated from *M. smegmatis* metabolite extracts. (PDF)

AUTHOR INFORMATION

Corresponding Authors

*R.P.: Tel: (402) 472-3039. Fax (402) 472-9402. E-mail: rpowers3@unl.edu.

*R.G.B.: Tel: (402) 472-8543. Fax (402) 472-9690. E-mail: rbarletta@unl.edu.

ORCID

Robert Powers: 0000-0001-9948-6837

Author Contributions

||D.D.M. and S.H. contributed equally.

Author Contributions

R.G.B. and R.P. designed the research; S.H. performed NMR experiments and statistical analysis; D.D.M. performed statistical analysis; H.K.C., R.J.F., G.R., and D.K.Z. prepared and analyzed the growth of the *M. smegmatis* cultures; S.H., D.D.M., and R.P. analyzed NMR and statistical data; S.H., D.D.M., D.K.Z., R.G.B., and R.P. analyzed metabolomics data; K.K. and R.J.F. generated proteomics data; K.K., R.J.F., and R.G.B. analyzed proteomics data; S.H., D.D.M., D.K.Z., R.G.B., and R.P. wrote the paper.

Notes

The authors declare no competing financial interest.

ACKNOWLEDGMENTS

We thank Dr. Renu Nandakumar and Dr. Nandakumar Madayiputhiya at the Proteomic and Metabolomics Core facility for providing the mudPIT proteomics data. This manuscript was supported in part by funds from the National Institute of Health (AI087668, P20 RR-17675, P30 GM103335), the USDA NIFA Station Animal Health Project (NEB 39-162), the American Heart Association (0860033Z), the UNL School of Veterinary Medicine and Biomedical Sciences, and the Nebraska Research Council. S.H. and R.J.F. were partially supported by O. Chacon's NIH grant (R21 AI087561) to standardize NMR techniques included in this publication. K.K. was supported by the Undergraduate Creative Activities and Research Experience (UCARE) program at UNL. The research was performed in facilities renovated with support from the National Institutes of Health (RR015468-01).

REFERENCES

- (1) *Global Tuberculosis Control Report*; World Health Organization, 2016.

- (2) Gengenbacher, M.; Kaufmann, S. H. E. Mycobacterium tuberculosis: success through dormancy. *FEMS Microbiol. Rev.* **2012**, *36* (3), 514–532.
- (3) Belanger, A. E.; Porter, J. C.; Hatfull, G. F. Genetic analysis of peptidoglycan biosynthesis in mycobacteria: characterization of a *ddlA* mutant of *Mycobacterium smegmatis*. *J. Bacteriol.* **2000**, *182* (23), 6854–6856.
- (4) Moat, A. G.; Foster, J. W.; Spector, M. P. Cell Structure and Function. In *Microbial Physiology*; John Wiley & Sons, Inc.: 2003; pp 277–349.
- (5) Brennan, P. J. Structure, function, and biogenesis of the cell wall of *Mycobacterium tuberculosis*. *Tuberculosis (Oxford, U. K.)* **2003**, *83* (1–3), 91–7.
- (6) Neuhaus, F. C. Selective inhibition of enzymes utilizing alanine in the biosynthesis of peptidoglycan. *Antimicrob. Agents Chemother.* **1968**, *1967* (7), 304–13.
- (7) Lambert, M. P.; Neuhaus, F. C. Factors affecting the level of alanine racemase in *Escherichia coli*. *J. Bacteriol.* **1972**, *109* (3), 1156–61.
- (8) Walsh, C. T. Enzymes in the D-alanine branch of bacterial cell wall peptidoglycan assembly. *J. Biol. Chem.* **1989**, *264* (5), 2393–6.
- (9) van Heijenoort, J. Biosynthesis of Bacterial Peptidoglycan Unit. In *Bacterial Cell Wall*, 1st ed.; Ghuyssen, J. M., Hakenbeck, R., Eds.; Elsevier Medical Press: Amsterdam, 1994; Vol. 27, pp 39–54.
- (10) Chacon, O.; Bermudez, L. E.; Zinniel, D. K.; Chahal, H. K.; Fenton, R. J.; Feng, Z.; Hanford, K.; Adams, L. G.; Barletta, R. G. Impairment of D-alanine biosynthesis in *Mycobacterium smegmatis* determines decreased intracellular survival in human macrophages. *Microbiology* **2009**, *155* (Pt 5), 1440–50.
- (11) Chacon, O.; Feng, Z.; Harris, N. B.; Caceres, N. E.; Adams, L. G.; Barletta, R. G. *Mycobacterium smegmatis* D-Alanine Racemase Mutants Are Not Dependent on D-Alanine for Growth. *Antimicrob. Agents Chemother.* **2002**, *46* (1), 47–54.
- (12) Halouska, S.; Chacon, O.; Fenton, R. J.; Zinniel, D. K.; Barletta, R. G.; Powers, R. Use of NMR metabolomics to analyze the targets of D-cycloserine in mycobacteria: role of D-alanine racemase. *J. Proteome Res.* **2007**, *6* (12), 4608–14.
- (13) Halouska, S.; Fenton, R. J.; Zinniel, D. K.; Marshall, D. D.; Barletta, R. G.; Powers, R. Metabolomics analysis identifies d-Alanine-d-Alanine ligase as the primary lethal target of d-Cycloserine in mycobacteria. *J. Proteome Res.* **2014**, *13* (2), 1065–76.
- (14) Milligan, D. L.; Tran, S. L.; Strych, U.; Cook, G. M.; Krause, K. L. The alanine racemase of *Mycobacterium smegmatis* is essential for growth in the absence of D-alanine. *J. Bacteriol.* **2007**, *189* (22), 8381–8386.
- (15) Awasthy, D.; Bharath, S.; Subbulakshmi, V.; Sharma, U. Alanine racemase mutants of *Mycobacterium tuberculosis* require D-alanine for growth and are defective for survival in macrophages and mice. *Microbiology (London, U. K.)* **2012**, *158* (2), 319–327.
- (16) Sassetti, C. M.; Boyd, D. H.; Rubin, E. J. Genes required for mycobacterial growth defined by high density mutagenesis. *Mol. Microbiol.* **2003**, *48* (1), 77–84.
- (17) Krzywinska, E.; Krzywinski, J.; Schorey, J. S. Naturally occurring horizontal gene transfer and homologous recombination in mycobacterium. *Microbiology (London, U. K.)* **2004**, *150* (6), 1707–1712.
- (18) Veyrier, F.; Pletzer, D.; Turenne, C.; Behr, M. A. Phylogenetic detection of horizontal gene transfer during the step-wise genesis of *Mycobacterium tuberculosis*. *BMC Evol. Biol.* **2009**, *9*, 196.
- (19) Snapper, S. B.; Melton, R. E.; Mustafa, S.; Kieser, T.; Jacobs, W. R., Jr. Isolation and characterization of efficient plasmid transformation mutants of *Mycobacterium smegmatis*. *Mol. Microbiol.* **1990**, *4* (11), 1911–9.
- (20) Miller, J. H. Determination of Viable Cell Counts: Bacterial Growth Curves. In *Experiments in Molecular Genetics*; Cold Spring Harbor Laboratory: Cold Spring Harbor, NY, 1972; pp 31–36.
- (21) Perkins, D. N.; Pappin, D. J. C.; Creasy, D. M.; Cottrell, J. S. Probability-based protein identification by searching sequence databases using mass spectrometry data. *Electrophoresis* **1999**, *20* (18), 3551–3567.
- (22) Zinniel, D. K.; Fenton, R. J.; Halouska, S.; Powers, R.; Barletta, R. G. Sample Preparation of *Mycobacterium tuberculosis* Extracts for Nuclear Magnetic Resonance (NMR) Metabolomic Studies. *J. Visualized Exp.* **2012**, *67*, e3673.
- (23) Halouska, S.; Zhang, B.; Gaupp, R.; Lei, S.; Snell, E.; Fenton, R. J.; Barletta, R. G.; Somerville, G. A.; Powers, R. Revisiting Protocols for the NMR Analysis of Bacterial Metabolomes. *Journal of Integrated OMICS* **2013**, *3*, 120–137.
- (24) Simpson, A. J.; Brown, S. A. Purge NMR: Effective and easy solvent suppression. *J. Magn. Reson.* **2005**, *175* (2), 340–346.
- (25) Hu, K. F.; Westler, W. M.; Markley, J. L. Simultaneous Quantification and Identification of Individual Chemicals in Metabolite Mixtures by Two-Dimensional Extrapolated Time-Zero H-1-C-13 HSQC (HSQC(0)). *J. Am. Chem. Soc.* **2011**, *133* (6), 1662–1665.
- (26) Hu, K.; Ellinger, J. J.; Chylla, R. A.; Markley, J. L. Measurement of absolute concentrations of individual compounds in metabolite mixtures by gradient-selective time-zero 1H-13C HSQC with two concentration references and fast maximum likelihood reconstruction analysis. *Anal. Chem.* **2011**, *83* (24), 9352–60.
- (27) Worley, B.; Powers, R. MVAPACK: A Complete Data Handling Package for NMR Metabolomics. *ACS Chem. Biol.* **2014**, *9* (5), 1138–1144.
- (28) Worley, B.; Powers, R. Simultaneous phase and scatter correction for NMR datasets. *Chemom. Intell. Lab. Syst.* **2014**, *131*, 1–6.
- (29) Worley, B.; Powers, R. Generalized adaptive intelligent binning of multiway data. *Chemom. Intell. Lab. Syst.* **2015**, *146*, 42–46.
- (30) Worley, B.; Halouska, S.; Powers, R. Utilities for quantifying separation in PCA/PLS-DA scores plots. *Anal. Biochem.* **2013**, *433* (2), 102–4.
- (31) Werth, M. T.; Halouska, S.; Shortridge, M. D.; Zhang, B.; Powers, R. Analysis of Metabolomic PCA Data using Tree Diagrams. *Anal. Biochem.* **2010**, *399* (1), 58–63.
- (32) Delaglio, F.; Grzesiek, S.; Vuister, G. W.; Zhu, G.; Pfeifer, J.; Bax, A. NMRPipe: a multidimensional spectral processing system based on UNIX pipes. *J. Biomol. NMR* **1995**, *6* (3), 277–93.
- (33) Johnson, B. A. Using NMRView to visualize and analyze the NMR spectra of macromolecules. *Methods in molecular biology* **2004**, *278*, 313–52.
- (34) Wishart, D. S.; Jewison, T.; Guo, A. C.; Wilson, M.; Knox, C.; Liu, Y.; Djoumbou, Y.; Mandal, R.; Aziat, F.; Dong, E.; Bouatra, S.; Sinelnikov, I.; Arndt, D.; Xia, J.; Liu, P.; Yallou, F.; Bjorn Dahl, T.; Perez-Pineiro, R.; Eisner, R.; Allen, F.; Neveu, V.; Greiner, R.; Scalbert, A. HMDB 3.0—The Human Metabolome Database in 2013. *Nucleic Acids Res.* **2013**, *41* (Database issue), D801–7.
- (35) Cui, Q.; Lewis, I. A.; Hegeman, A. D.; Anderson, M. E.; Li, J.; Schulte, C. F.; Westler, W. M.; Eghbalnia, H. R.; Sussman, M. R.; Markley, J. L. Metabolite identification via the Madison Metabolomics Consortium Database. *Nat. Biotechnol.* **2008**, *26* (2), 162–4.
- (36) Akiyama, K.; Chikayama, E.; Yuasa, H.; Shimada, Y.; Tohge, T.; Shinozaki, K.; Hirai, M. Y.; Sakurai, T.; Kikuchi, J.; Saito, K. PRIME: a Web site that assembles tools for metabolomics and transcriptomics. *In Silico Biol.* **2008**, *8* (3–4), 339–45.
- (37) Okuda, S.; Yamada, T.; Hamajima, M.; Itoh, M.; Katayama, T.; Bork, P.; Goto, S.; Kanehisa, M. KEGG Atlas mapping for global analysis of metabolic pathways. *Nucleic Acids Res.* **2008**, *36* (WebServer issue), W423–6.
- (38) Caspi, R.; Foerster, H.; Fulcher, C. A.; Kaipa, P.; Krummenacker, M.; Latendresse, M.; Paley, S.; Rhee, S. Y.; Shearer, A. G.; Tissier, C.; Walk, T. C.; Zhang, P.; Karp, P. D. The MetaCyc Database of metabolic pathways and enzymes and the BioCyc collection of Pathway/Genome Databases. *Nucleic Acids Res.* **2007**, *36* (Database issue), D623–31.
- (39) Bylesjo, M.; Rantalainen, M.; Cloarec, O.; Nicholson, J. K.; Holmes, E.; Trygg, J. OPLS discriminant analysis: combining the

strengths of PLS-DA and SIMCA classification. *J. Chemom.* **2006**, *20* (8–10), 341–351.

(40) Woodruff, P. J.; Carlson, B. L.; Siridechadilok, B.; Pratt, M. R.; Senaratne, R. H.; Mougous, J. D.; Riley, L. W.; Williams, S. J.; Bertozzi, C. R. Trehalose is required for growth of *Mycobacterium smegmatis*. *J. Biol. Chem.* **2004**, *279* (28), 28835–43.

(41) Copie, V.; Faraci, W. S.; Walsh, C. T.; Griffin, R. G. Inhibition of alanine racemase by alanine phosphonate: detection of an imine linkage to pyridoxal 5'-phosphate in the enzyme-inhibitor complex by solid-state ¹⁵N nuclear magnetic resonance. *Biochemistry* **1988**, *27* (14), 4966–70.

(42) Lambert, M. P.; Neuhaus, F. C. Mechanism of D-cycloserine action: alanine racemase from *Escherichia coli* W. *J. Bacteriol.* **1972**, *110* (3), 978–87.

(43) Silverman, R. B. The potential use of mechanism-based enzyme inactivators in medicine. *J. Enzyme Inhib.* **1988**, *2* (2), 73–90.

(44) Feng, Z.; Caceres, N. E.; Sarath, G.; Barletta, R. G. *Mycobacterium smegmatis* L-alanine dehydrogenase (Ald) is required for proficient utilization of alanine as a sole nitrogen source and sustained anaerobic growth. *J. Bacteriol.* **2002**, *184* (18), 5001–5010.

(45) Thompson, R. J.; Bouwer, H. G. A.; Portnoy, D. A.; Frankel, F. R. Pathogenicity and immunogenicity of a *Listeria monocytogenes* strain that requires D-alanine for growth. *Infect. Immun.* **1998**, *66* (8), 3552–3561.

(46) Kwak, M.-S.; Lee, S.-G.; Jeong, S.-C.; Suh, S.-H.; Lee, J.-H.; Jeon, Y.-J.; Kim, Y.-H.; Sung, M.-H. Screening and taxonomic characterization of D-amino acid aminotransferase-producing thermophiles. *Sanop Misaengmul Hakhoechi* **1999**, *27* (3), 184–190.

(47) Taylor, P. P.; Fotheringham, I. G. Nucleotide sequence of the *Bacillus licheniformis* ATCC 10716 *dat* gene and comparison of the predicted amino acid sequence with those of other bacterial species. *Biochim. Biophys. Acta, Gene Struct. Expression* **1997**, *1350* (1), 38–40.

(48) Berger, B. J.; English, S.; Chan, G.; Knodel, M. H. Methionine regeneration and aminotransferases in *Bacillus subtilis*, *Bacillus cereus*, and *Bacillus anthracis*. *J. Bacteriol.* **2003**, *185* (8), 2418–2431.

(49) Kobayashi, J.; Shimizu, Y.; Mutaguchi, Y.; Doi, K.; Ohshima, T. Characterization of D-amino acid aminotransferase from *Lactobacillus salivarius*. *J. Mol. Catal. B: Enzym.* **2013**, *94*, 15–22.

(50) Lee, S.-G.; Hong, S.-P.; Song, J. J.; Kim, S.-J.; Kwak, M.-S.; Sung, M.-H. Functional and structural characterization of thermostable D-amino acid aminotransferases from *Geobacillus* spp. *Appl. Environ. Microbiol.* **2006**, *72* (2), 1588–1594.

(51) Halouska, S.; Fenton, R. J.; Zinniel, D. K.; Marshall, D. D.; Barletta, R. G.; Powers, R. Metabolomics analysis identifies D-Alanine-D-Alanine ligase as the primary lethal target of D-cycloserine in mycobacteria. *J. Proteome Res.* **2014**, *13* (2), 1065–1076.

(52) Amon, J.; Braeu, T.; Grimath, A.; Haenssler, E.; Hasselt, K.; Hoeller, M.; Jessberger, N.; Ott, L.; Szoekoel, J.; Titgemeyer, F.; Burkovski, A. Nitrogen control in *Mycobacterium smegmatis*: nitrogen-dependent expression of ammonium transport and assimilation proteins depends on the OmpR-type regulator GlnR. *J. Bacteriol.* **2008**, *190* (21), 7108–7116.

(53) Jenkins, V. A.; Barton, G. R.; Robertson, B. D.; Williams, K. J. Genome wide analysis of the complete GlnR nitrogen-response regulon in *Mycobacterium smegmatis*. *BMC Genomics* **2013**, *14*, 301.

(54) Williams, K. J.; Jenkins, V. A.; Barton, G. R.; Bryant, W. A.; Krishnan, N.; Robertson, B. D. Deciphering the metabolic response of *Mycobacterium tuberculosis* to nitrogen stress. *Mol. Microbiol.* **2015**, *97* (6), 1142–1157.

(55) Galamba, A.; Soetaert, K.; Buysens, P.; Monnaie, D.; Jacobs, P.; Content, J. Molecular and biochemical characterisation of *Mycobacterium smegmatis* alcohol dehydrogenase C. *FEMS Microbiol. Lett.* **2001**, *196* (1), 51–6.

(56) Feehily, C.; Karatzas, K. A. G. Role of glutamate metabolism in bacterial responses towards acid and other stresses. *J. Appl. Microbiol.* **2013**, *114* (1), 11–24.